N94-24216

PRELIMINARY ANALYSIS OF AMPLITUDE AND PHASE FLUCTUATIONS IN THE JAPE MULTIPLE TONE DATA TO DISTANCES OF 500 METERS

James Rogers, Radomir Sokolov
Michigan Technological University
1400 Townsend Drive
Houghton, Michigan 49931

Daniel Hicks, Lloyd Cartwright
AMSTA-JCS
U.S. Army TARDEC
Warren, Michigan 48397-5000

59-71

20168l

p. 14

INTRODUCTION AND PURPOSE

The JAPE short range data provide a good opportunity for studying phase and amplitude fluctuations of acoustic signals in the atmosphere over distances of several hundred meters. Several factors contribute to the usefulness of these data: extensive meteorological measurements were made, controlled sources were used, the data were recorded with a high dynamic range digital system that preserved phase information and a significant number of measurement points were obtained allowing both longitudinal and transverse studies. Further, Michigan Tech, in cooperation with the U.S. Army TARDEC, has developed phase tracking algorithms for studying vehicle acoustic signals. These techniques provide an excellent tool for analyzing the amplitude and phase fluctuations of the JAPE data.

The results of studies such as those reported here have application at several levels: the mechanisms of signal amplitude and phase fluctuations in propagating acoustic signals are not well understood nor are the mathematical models highly developed, acoustic arrays depend strongly on signal coherence and signal amplitude stability in order to perform to their design specifications and active noise control implementation in regions considerably removed from the primary and secondary sources depends upon signal amplitude and phase stability.

Work reported here is preliminary in nature but it does indicate the utility of the phase tracking and amplitude detection algorithms. The results obtained indicate that the phase fluctuations of the JAPE continuous multiple tone data (simultaneous transmission of 80, 200 and 500 Hz) are in general agreement with existing theories but the amplitude fluctuations are seen to be less well behaved and show less consistency.

THE MEASUREMENT SITE AND DATA ANALYZED

Figure 1 is a sketch depicting the short range propagation experiment site. The separation distance of the north and south towers is 1000 meters and the microphone array is located midway between them. The data analyzed here were from trial 033102 at time 22:50 (MDT). The speaker was located at the base of the north tower. Microphone spacing along the line was 100 meters while a variety of spacings were used for the array as shown in the figure. The numbering scheme used in the figure does not correspond with the channel numbers assigned during the experiment. Since some of the channels were not useful, the microphone at the base of the North tower was overdriven; while other microphones did not provide signals, the microphones were renumbered as indicated in the figure. Thus neither microphone 5 nor 6

has a corresponding microphone in the typical arrangement for a pair of microphones, one on the ground and one located one meter above that. This numbering arrangement seen in the figure facilitates later plots.

Two seconds of raw data are shown in Figure 2 where the bottom trace is the acoustic signal recorded at 400 m from the north tower base and the traces above that are from 300, 200, and 100 m respectively. The vertical scale of the traces is uncalibrated but it is the same for all traces. Wind noise is the principal feature of the traces but there is clearly a signal present. The three simultaneous tones at 80, 200 and 500 Hz present one hundred sixty cycles over the 2 second time span of the figure and are evidenced by the decreasing width of the signal trace from the top of the figure to the bottom. The trace corresponding to the 300 m distance shows little effects of wind when compared to the other three traces. No reason is known for this feature. The winds at the dirt site west tower were approximately 2 m/s and 3 m/s at 2 and 10 m elevations respectively. The direction was approximately 220 degrees.

The FFT amplitude spectra from the data in Figure 2 are shown in Figure 3, where the vertical scale is not calibrated. Background noise and wind noise are clearly evident in this figure as are the three simultaneous tones. In order to improve resolution of the tonal peaks the time series data record length transformed was 2.5 seconds. A principal advantage to analyzing the simultaneous tone data instead of data with single tones is that comparisons of the phase and amplitude fluctuations for a sequence of separate tones depend on the stability of the meteorological conditions. However, analysis of simultaneous tones does not require this. A trade off in this choice however is that the power in each single transmitted tone can be determined by the total system power available while for multiple tones the power in each tone is necessarily only a portion of the total system power available. Thus the signal to noise for each tone is worse for the multiple tone measurement.

PHASE AND AMPLITUDE EXTRACTION

Each of the three tones was analyzed separately but with a common algorithm. First the data were passed through an eight pole band pass filter with a 2.5 Hz bandwidth centered on the tone of interest. The filter had a linear phase characteristic throughout the passband. After a real signal to analytic signal conversion using an FIR Hilbert transformation, the signal amplitude was extracted. The next step in the analysis was phase tracking the received tone. Figure 4 is a conceptual diagram of the amplitude and phase extraction process.

Since the phase detector in the phase locked loop is sensitive to signal amplitude, the amplitude information previously obtained was used to restore the signal to a constant amplitude prior to phase tracking. The natural frequency of the phase lock loop was 0.75 Hz. In order to remove the signal component at twice the VCO frequency which is present after the phase detector an adaptive notch filter operating at twice the VCO instantaneous frequency was used. This filter is considerably above the bandwidth of the signal of interest and it is expected to have no effect on the phase information from the loop. It was possible to monitor the phase error of the tracking loop and to observe that phase lock was easily maintained with only insignificant phase errors. The final step in the phase analysis was removal of the difference frequency between the free running VCO and the frequency of the tone used in the experiment. It was observed that the values 80, 200 and 500 Hz were nominal and that the actual measurement frequencies were different from these values by a fraction of a Hz.

SPATIAL CHARACTERISTICS OF AMPLITUDE AND PHASE DATA

The theoretical development of the meteorological effects on propagating acoustic signals has roots in the work of Karavainikov, Chernov and Tatarskii (refs 1,2,3). Daigle, Piercy and Embleton (ref 4) reviewed the theory pertinent to line of sight propagation through atmospheric turbulence. McBride, Bass, Raspet and Gilbert approached the problem of sound scattering in atmospheric turbulence by developing a computer simulation of the effects of small scale turbulence (ref 5). The theory (ref 4) assumes homogeneous and isotropic turbulence. Large atmospheric eddies are formed by instabilities in the

boundary layer near the ground and additional instability produces progressively smaller eddies until they are dissipated by viscosity. After assuming a Gaussian turbulence distribution they develop expressions for the log-amplitude and phase fluctuations for pure tones propagated through a turbulent atmosphere near the ground. Only a brief overview of their presentation is given here to define the quantities which we present in later figures.

The log-amplitude, $M_{i,n}$, for the i-th microphone at the n-th time sample is

$$M_{i,n} = \ln\left(\frac{A_{i,n}}{A_{i,0}}\right) \qquad (1)$$

where $A_{i,n}$ represents amplitude.
The average amplitude, $A_{i,0}$, over N samples at a fixed distance, is

$$A_{i,0} = \frac{1}{N} * \sum_{n=1}^{n=N} A_{i,n} \qquad (2)$$

and mean square log-amplitude is given in Equation 3

$$\overline{M_{i,n}^2} = \frac{1}{N} * \sum_{n=1}^{n=N} M_{i,n}^2 \qquad (3)$$

The phase structure function calculation is shown in Equation 4 of reference 4. The second term takes into account the mean phase difference of the measured data which may not be zero.

$$\overline{\Phi^2} = \frac{1}{N} \sum_{n=1}^{n=N} (\phi_{i,n} - \phi_{j,n})^2 - \left(\frac{1}{N} \sum_{n=1}^{n=N} (\phi_{i,n} - \phi_{j,n})\right)^2 \qquad (4)$$

$\Phi_{i,n}$ is the phase of the i-th microphone at the n-th sample.

Figure 5 shows sixteen seconds of the amplitude fluctuations for each of the three frequencies at distances of 100, 200, 300 and 400 m. Figure 6 presents the corresponding phase fluctuations for these frequencies and distances. The vertical scale on the amplitude plots is uncalibrated but it is the same for all plots. The vertical scale on the phase plots is the same for all plots and it is in radians. With some effort it is possible to clearly discern a pattern in the phase data: for all of the plots at a given frequency the least phase fluctuations occur at 100 m and the fluctuations increase with increasing distance. Another intriguing feature of the phase data for 80 and 200 Hz is the rather cyclic and regular nature of the fluctuations. For example the five second interval between 1 and 6 seconds on the 200 Hz plot for a distance of 400 m has regular fluctuations at a frequency of approximately 1.4 Hz. No explanation is presented for this character.

Figure 7 shows the logarithm of the average signal amplitude at three frequencies vs distance from the speaker. Also shown in the figure is a straight line with a slope of minus one which would be expected for signals with principal attenuation due to geometrical spreading. There is sufficient agreement between the trend of the data and the straight line that simple spreading is presumed to be the principal

attenuation mechanism at 500 Hz. However, there is some inconsistency in the data for 80 and 200 Hz where the signal loss appears to be less than that predicted by geometrical spreading.

Figure 8 shows mean square log-amplitude as a function of longitudinal distance from the source. The averaging time was 16 seconds. The plot generally shows increasing log-amplitude fluctuations with distance. Examination of the variations of signal amplitude with time shown earlier in Figure 5 suggests that 4 seconds is too short a time for calculating the average behavior and that 16 seconds may be more appropriate.

Figure 9 shows the dependence of mean square phase fluctuations as a function of longitudinal distance. There is a clear increase in phase fluctuations with longitudinal distance as is predicted by equation (2) (ref 4) which shows a linear dependence upon longitudinal distance. Also, increasing fluctuations with frequency are expected from the theory (refs 2,3).

All of the phase difference fluctuations between the microphones are portrayed in figure 10. The vertical axis is mean square phase fluctuations and it is scaled in radians. The two horizontal indexes correspond to microphone numbers which were indicated in Figure 1. Considerable information can be discerned from the figure. The intersection of microphone 12 with microphone 11 shows a small value for phase difference; microphone 12 is located directly above microphone 11 at an elevation of 1 m. The intersection of microphone 12 with microphone 10 shows a larger value for phase difference; both microphones are elevated 1 m and their horizontal separation is 1 m. Since the 8-9 and the 9-8 phase differences are the same, the redundant data are not shown in Figure 10. A general interpretation of the figure is that the phase fluctuations between microphones tend to increase with microphone separation distance. This trend is not seen in the first four microphones since their separation is 100 m which is considerably beyond the phase coherence predicted by the theory.

Figure 11 shows the phase coherence of the microphones in the transverse array located at 500 m. It is a plot of the mean square phase fluctuations between microphones in the array as a function of the logarithm of their separation distance. Also shown in the figure is a line with a slope of 5/3 which is predicted by theory (see equation 5). There is general agreement between the data and the theory for the shorter distances.

$$\overline{\phi}^2 = const * (\frac{f}{2*\pi *c})^2 *L*b^{\frac{5}{3}} *C \qquad (5)$$

L   source -microphone distance
b   separation between two microphones
f   frequency
c   speed of sound
C   turbulence characteristic

Numerical analysis of the data in Figure 11 shows the 5/3 law is approximately valid for separation distances up to 3 m. However, the 5/3 law is less well adhered to for a signal frequency of 200 Hz (see Figure 12). Further increasing the signal frequency to 500 Hz shows even less adherence to the 5/3 law relationship. This observation shows that the outer scale of turbulence can be calculated when the range of validity of separation distance is estimated. We have not analyzed the meteorological data to determine the apparent fluctuations in the atmospheric index of refraction but these too would be expected to produce an outer scale on the order of a few meters. Consequently, at larger distances the phase fluctuations are not expected to follow a 5/3 relation.

DISCUSSION AND CONCLUSIONS

Given the rather large amount of unwanted noise present with each of the tones it is desirable to restrict the analysis bandwidth to ensure the greatest signal to noise for the analysis. However, a compromise is required in order to ensure that significant signal amplitude and phase fluctuations are allowed to pass through the system. The 2.5 Hz filter was a choice made for these preliminary results. Initial investigations indicated that this bandwidth is not too restrictive and that significant information is available from the analysis algorithm described above. Additional studies will be required to determine if there is a better choice for the analysis bandwidth. However, there is no hard threshold where the results change from useless to useful and a certain amount of judgment is therefore required in selection of the "proper" analysis bandwidth.

Another issue that is not addressed in the existing theory that requires additional study is determining the amount of data that should be used to calculate the RMS amplitude and phase fluctuations. It was seen earlier that the results from a 16 second average and from a 4 second average were quite different. This should be expected if one considers the variations in the amplitude vs time and phase vs time curves shown in Figures 5 and 6 respectively. The decision on the "proper" averaging time must be made using judgment based upon the time variability of these curves as there is no theory to provide adequate guidance on this issue.

The data analysis presented here is preliminary. It is necessary to examine additional data in order to better characterize the temporal and spatial variations of the acoustic data. The meteorological data too should be further examined so statistical parameters can be determined. Finally, an assesment of fluctuating amplitude and phase effects on microphone array performance and on the behavior of the active noise control (ACN) systems should be made.

REFERENCES

1.   Karavainikov, V. N.: "Fluctuations of amplitude and phase in a spherical wave," Aakust. Zh. 3, 175-186, 1957.

2.   Chernov, L. A.: Wave Propagation in a Random Medium, McGraw-Hill, New York, 1960.

3.   Tatarskii, I.: The Effects of the Turbulent Atmosphere on Wave Propagation, Ketter, Jerusalem, 1971.

4.   Daigle, G. A., Piercy, J. E. and Embleton, T. F. W.: Line-of-sight Propagation Through Atmospheric Turbulence Near the Ground, Journal of the Acoustical Society of America, Vol. 74, No. 5, Nov. 1983, pp 1505-1513.

5.   McBride, W., Bass, H. E., Raspet, R., Gilbert, K. : Scattering of Sound by Atmospheric Turbulence: A Numerical Simulation Above a Complex Impedance Boundary, Journal of the Acoustical Society of America, vol. 90, No. 6, Dec. 1991, pp 3314-3325.

Short Range Propagation Experiments

White Sands Missile Range, July 1991

S   N

1.0 meter above the ground

32 meters

13

12

10 11

8 9

1m

7

2m

6

4m

5

8m

4   3   2   Mic. 1   100m 0

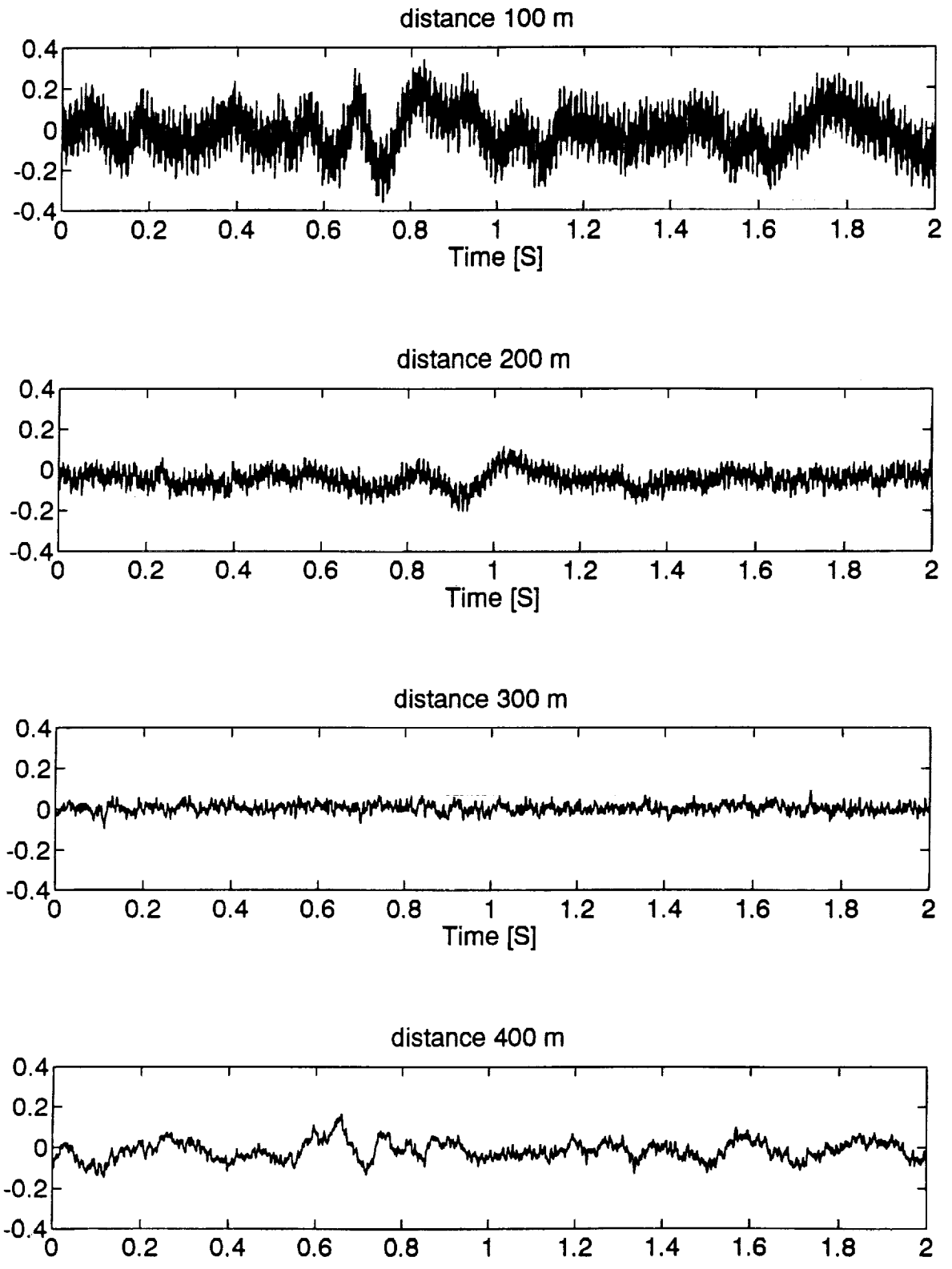Figure   1   Short range propagation site
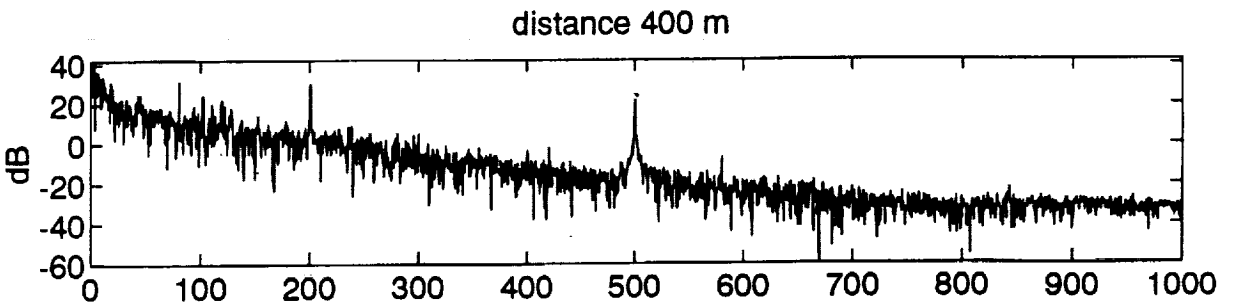
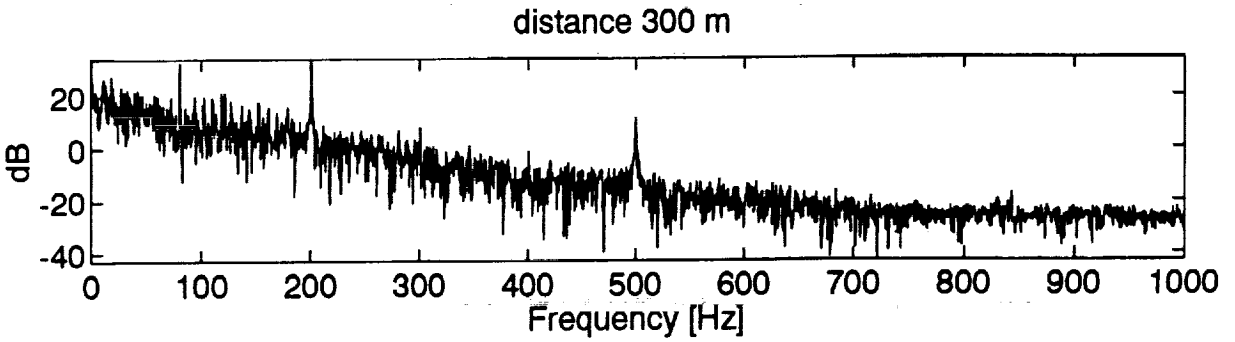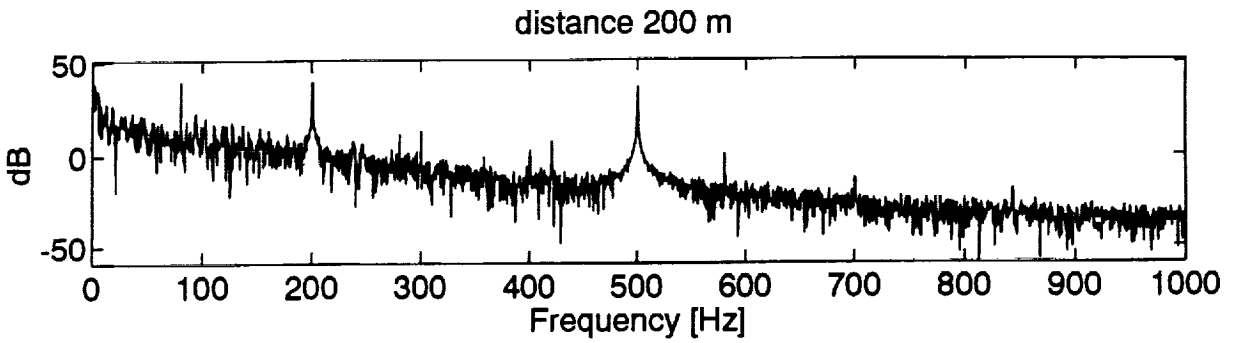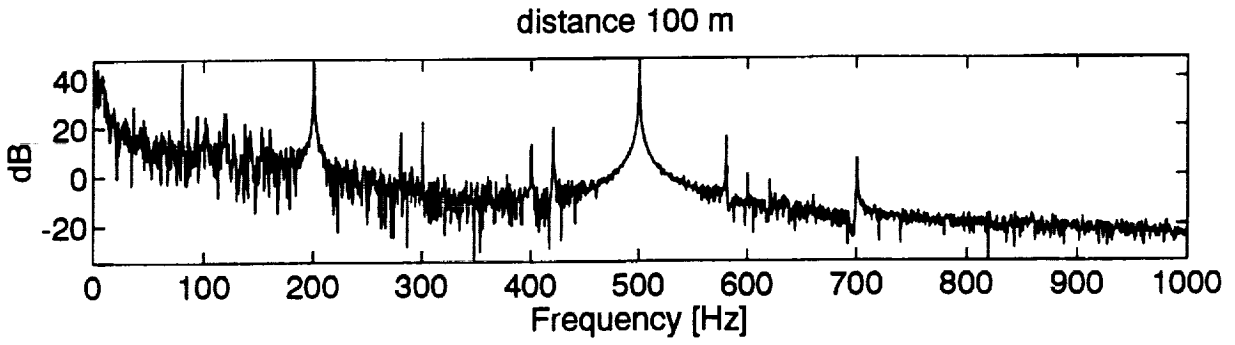Figure 2   Recorded acoustic signals (100 - 400 m), trial No:03310 2.

Figure 3 FFT spectra from the data in Figure 2.
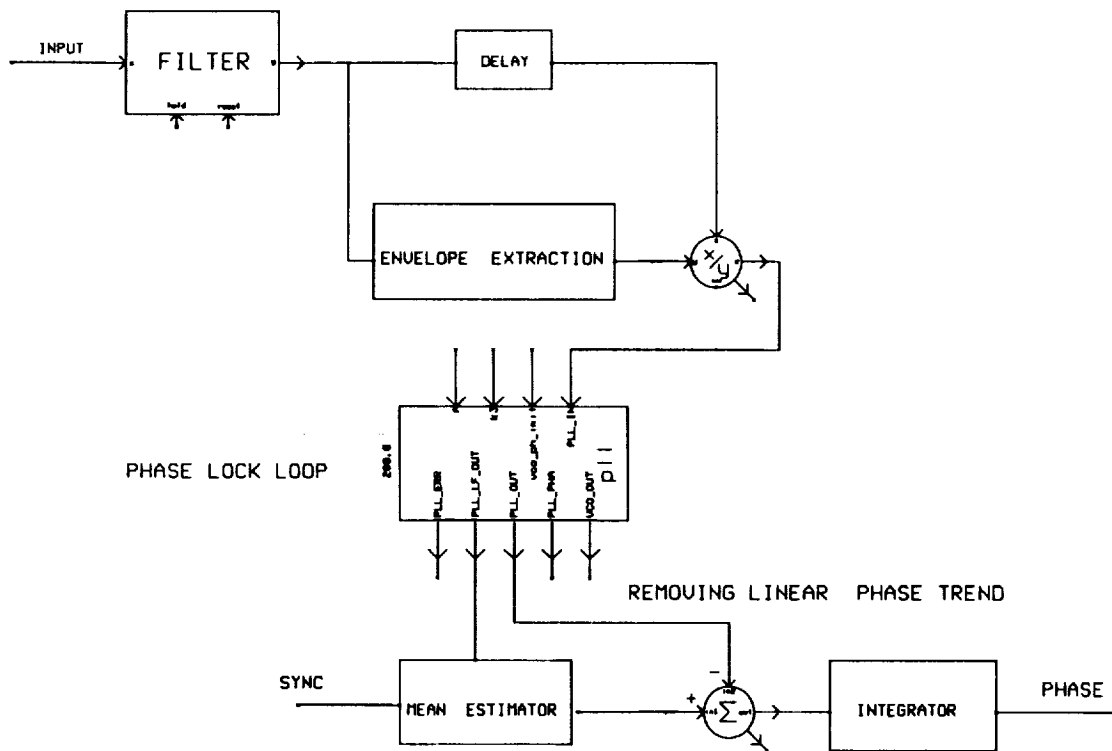
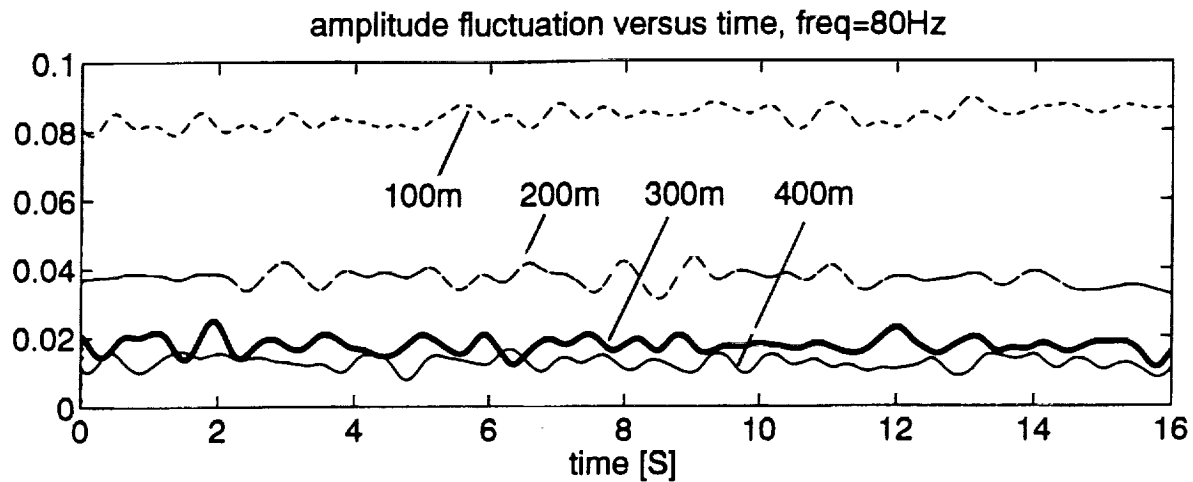Figure 4   Conceptual diagram of the amplitude and phase extraction process.

amplitude fluctuation versus time, freq=80Hz

100m   200m   300m   400m

amplitude fluctuation versus time, freq=200Hz

amplitude fluctuation versus time, freq=500Hz
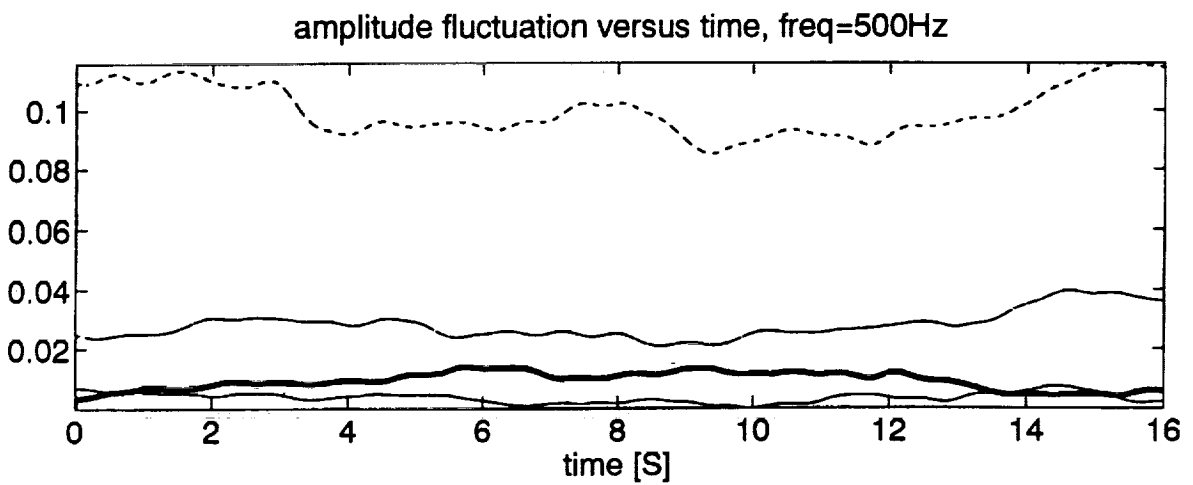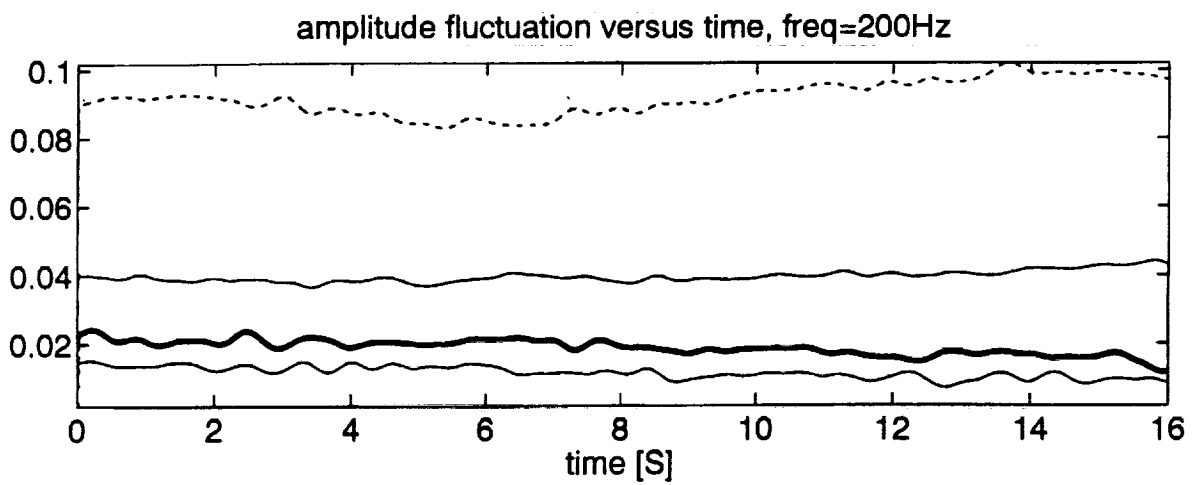
Figure 5   Amplitude fluctuations at distances 100 m - 400 m
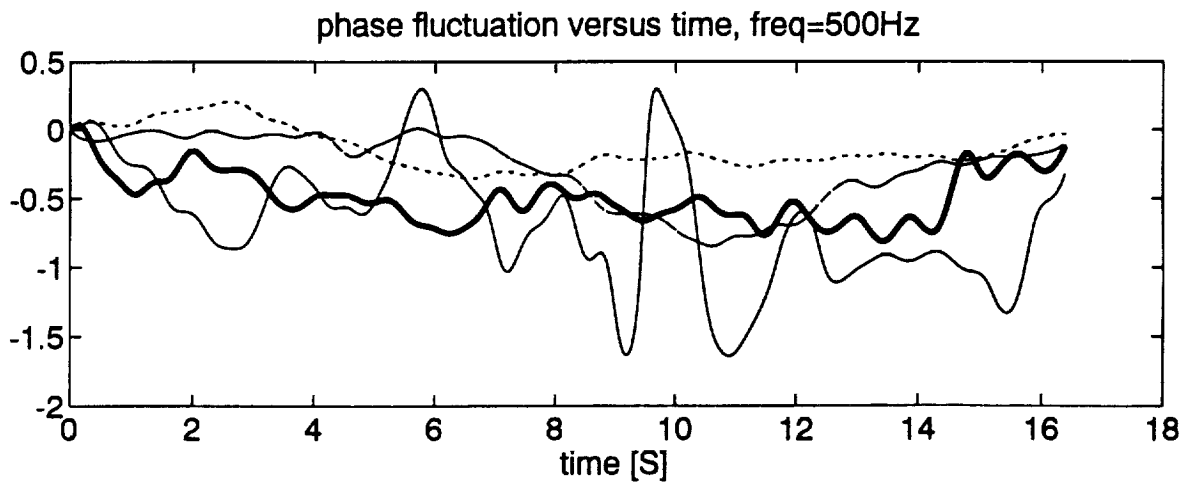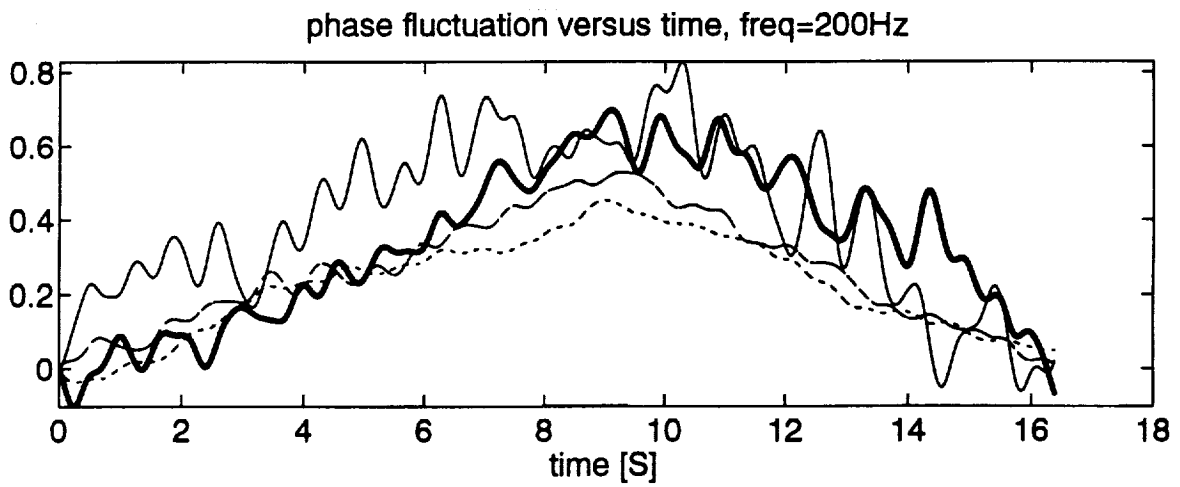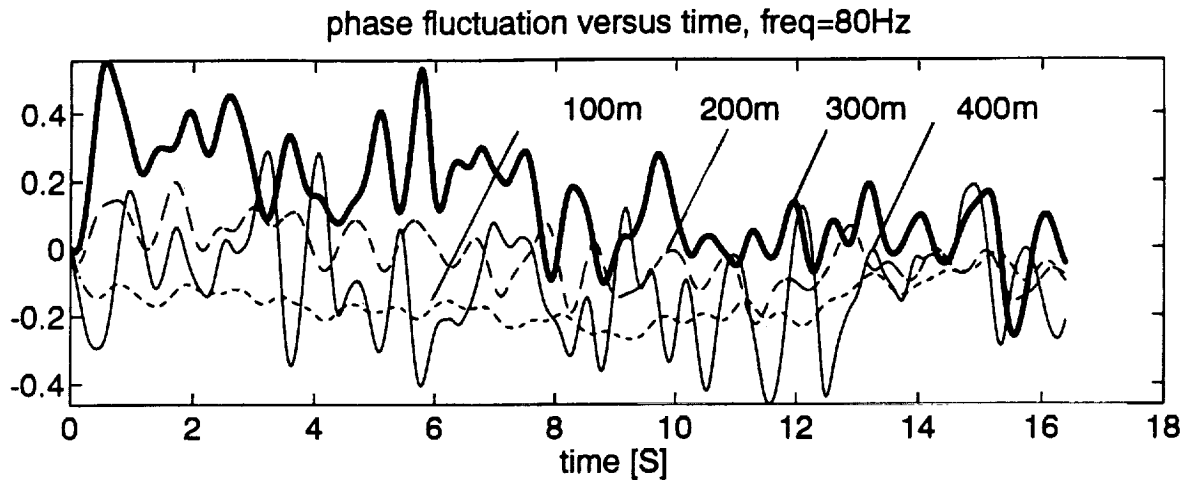
Figure 6   Phase fluctuations at distances 100 m - 400 m
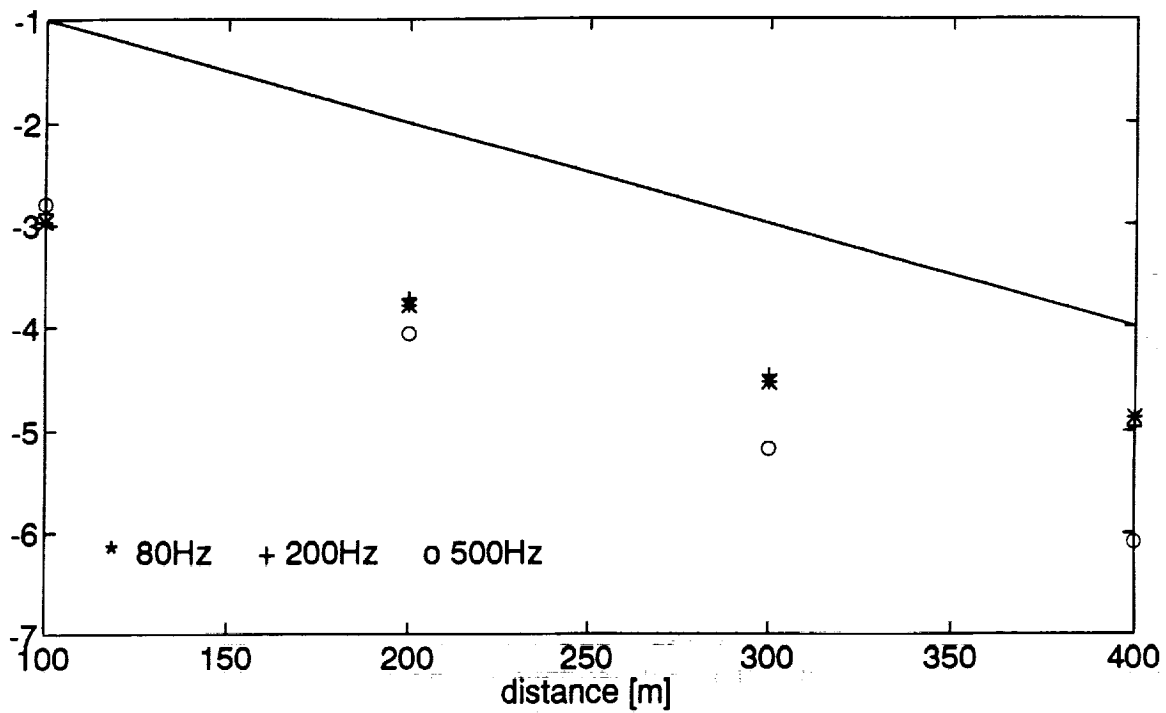
Figure 7   Log-average amplitude at different microphone positions.
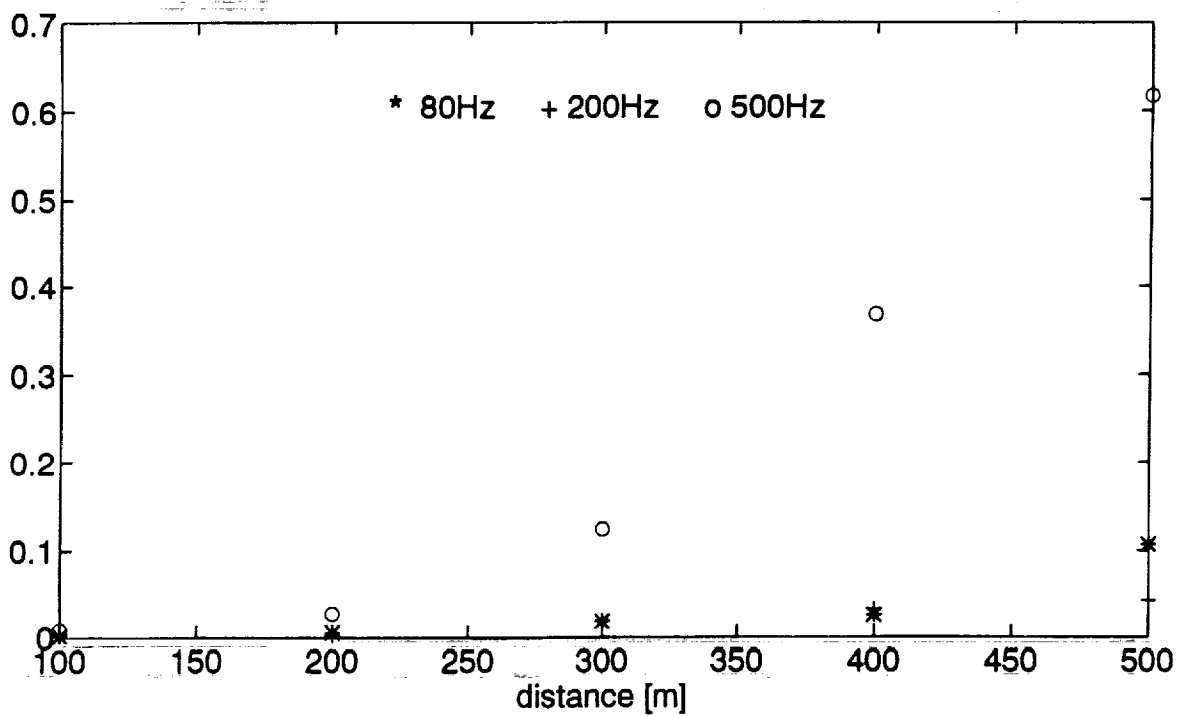
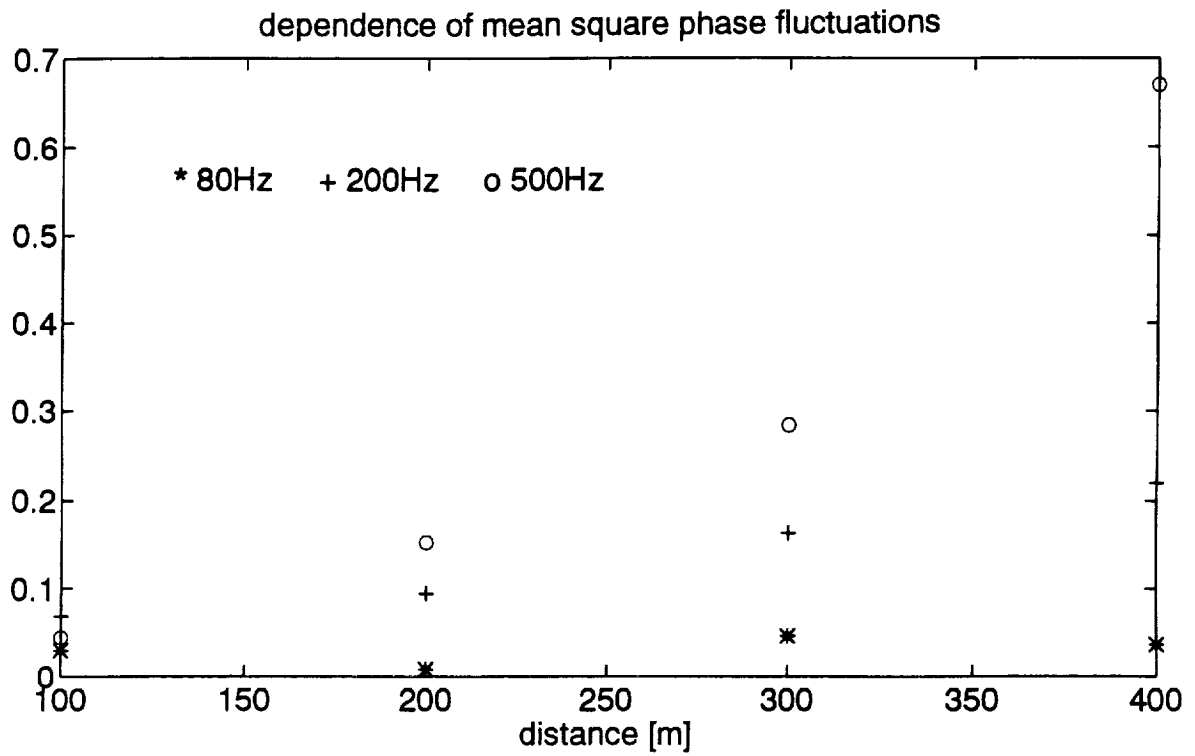Figure 8   Mean square log-amplitude fluctuations, time_average=16s

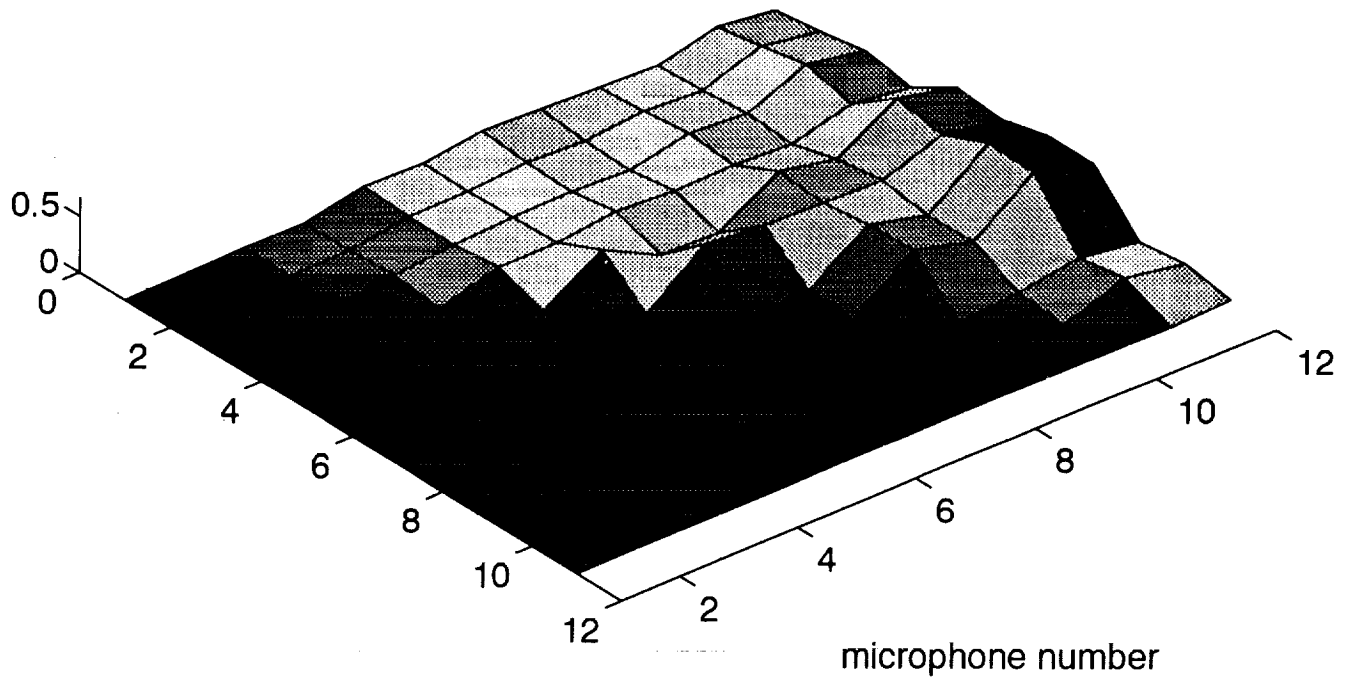Figure 9   Mean square phase fluctuations versus distance.

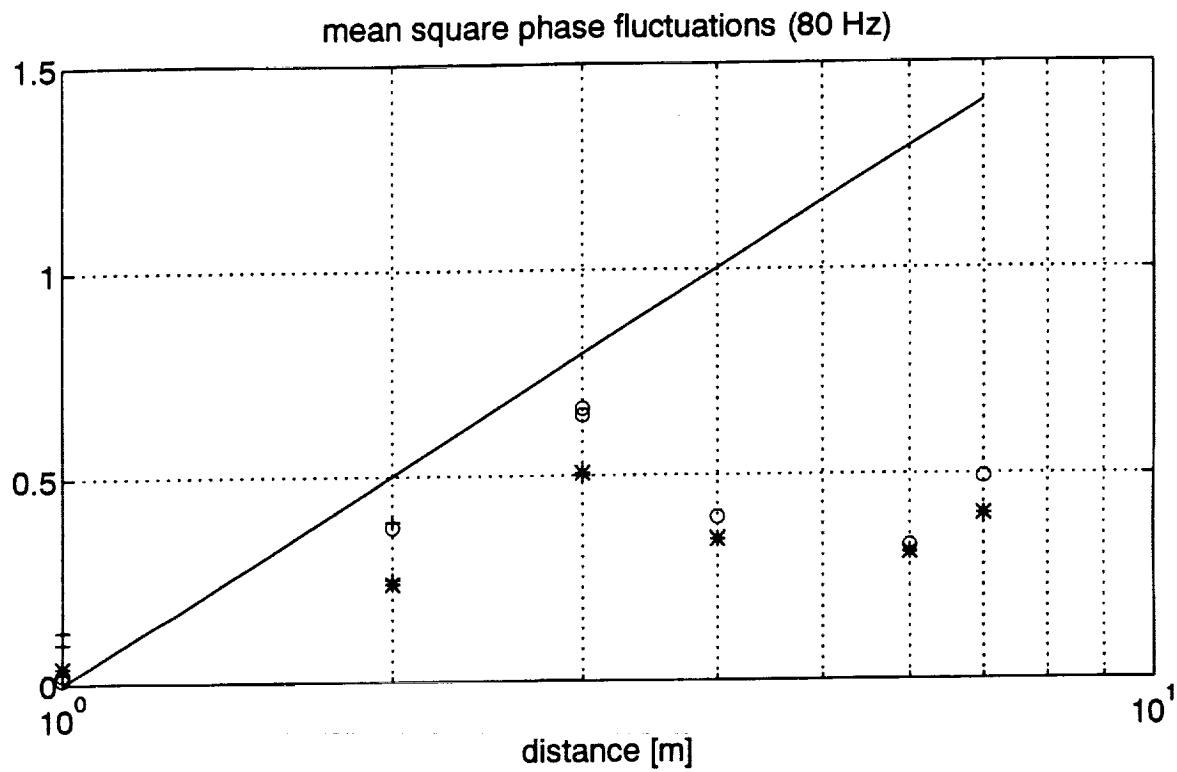Figure 10   Mean square phase difference between microphones.

mean square phase fluctuations (80 Hz)

distance [m]

Figure 11   Mean square phase fluctuations in the transverse array.

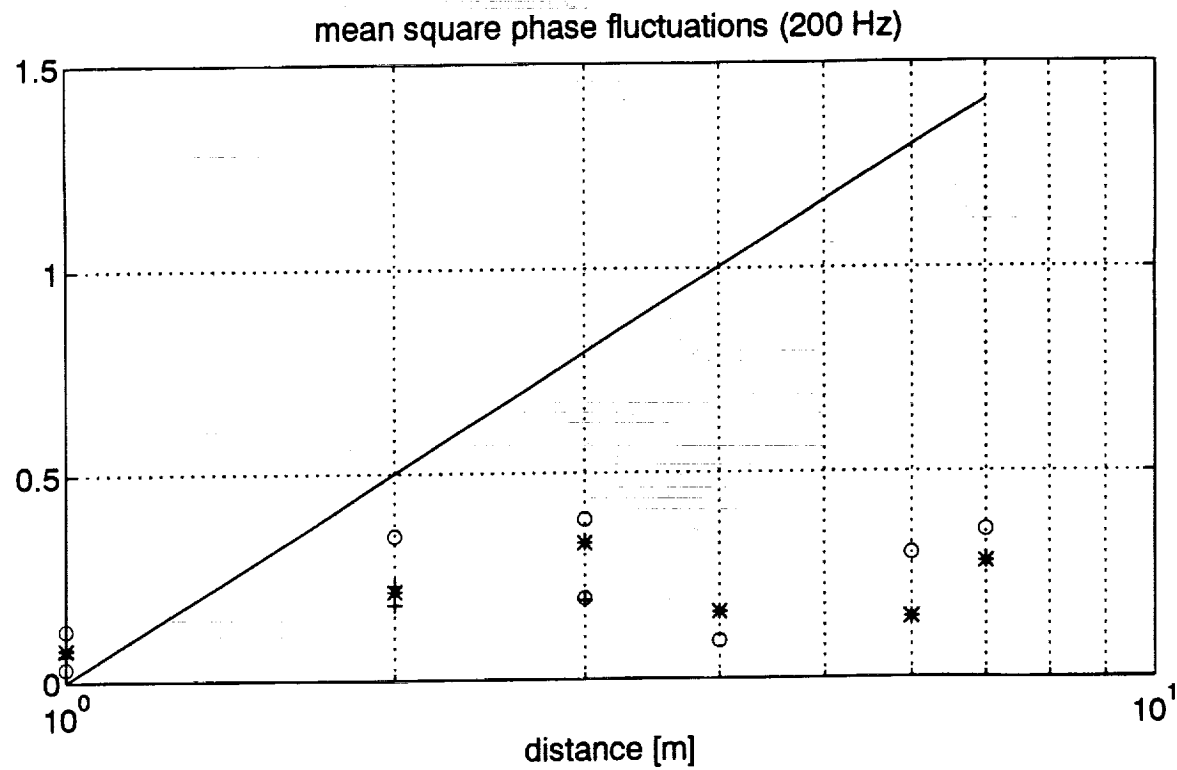## mean square phase fluctuations (200 Hz)

distance [m]

Figure 12   Mean square phase fluctuations in the transverse array.

106